Project: **839**

Project title: **Quantifying Aerosol-Cloud-Climate Effects by Regime (QUAERERE)**

Project lead: **Johannes Quaas**

Report period: **1.1.2017 - 31.12.2017**

The goal of the ERC-funded QUAERERE project is a better assessment of the effective radiative forcing by aerosol-cloud interactions mainly from satellite data, with support from modelling.

In some deviation from the initial plans, we carried out in the reporting period mainly two studies:

(i) a deepened understanding of the adjustments of liquid-water clouds via the "lifetime effect". This follows up on the studies already reported on last year, where the autoconversion rate was scaled down. In a more realistic setting, the threshold in effective radius when autoconversion starts is now considered (Fig. 1; see also Suzuki et al., 2013). As seen, a more realistic (larger) critical effective radius leads to a more realistic pattern of warm-rain fraction.

(ii) we investigated the radiative forcing by aerosol-radiation interactions ("direct effect") that to a large extent is affected by aerosol swelling (e.g. Quaas et al., 2010). The idea was to make use of the subgrid-scale variability of relative humidity (e.g., Quaas, 2012). Aerosol optical properties (aerosol optical depth in particular) are now considered from the probability density function (PDF) of the relative humidity in clear sky, drawing from the PDF consistent with the model's cloud scheme (stochastic parameterisation). This is useful since aerosol swelling is strongly non-linear in relative humidity. The results are summarized in Table 1. Many of the relevant quantities change. The most striking result is that the present day – pre-industrial difference in clear-sky radiation ("aerosol direct effect") changes by more than 50%. This is because anthropogenic aerosols are disproportionally hydrophilic. The results are submitted in Petersik et al. (2018).

References

Suzuki, K., J.-C. Golaz, and G. L. Stephens (2013), Evaluating cloud tuning in a climate model with satellite observations, Geophys. Res. Lett., 40, 4464–4468, doi:10.1002/grl.50874

***Mülmenstädt, J., O. Sourdeval,** J. Delanoë, and **J. Quaas**, Frequency of occurrence of rain from liquid-, mixed- and ice-phase clouds derived from A-Train satellite retrievals, Geophys. Res. Lett., 42, 6502-6509, doi:10.1002/2015GL064604, 2015.*

***Petersik, P., M. Salzmann, J. Kretzschmar, R. Cherian, D. Mewes,** and **J. Quaas**, Subgrid-scale variability of clear-sky relative humidity and forcing by aerosol-radiation interactions in an atmosphere model, Atmos. Chem. Phys. Discuss., submitted (2018).*

***Quaas, J.**, B. Stevens, U. Lohmann, and P. Stier, Interpreting the cloud cover - aerosol optical depth relationship found in satellite data using a general circulation model, Atmos. Chem. Phys., 10, 6129-6135, doi:10.5194/acp-10-6129-2010, 2010.*

***Quaas, J.**, Evaluating the "critical relative humidity" as a measure of subgrid-scale variability of humidity in general circulation model cloud cover parameterizations using satellite data, J. Geophys. Res., 117, D09208, doi:10.1029/2012JD017495, 2012.*

Figures

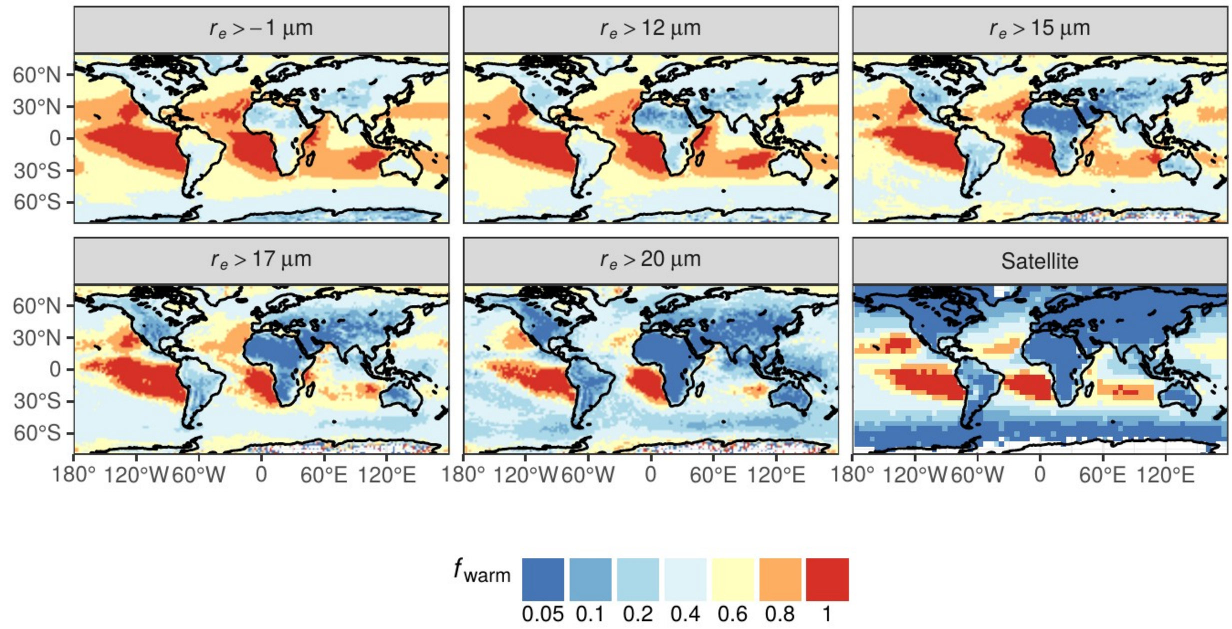

Fig. 1: Warm-rain fraction in the ECHAM6-HAM2 model using varying thresholds in cloud droplet effective radius in the autoconversion parameterisation in comparison to the satellite-derived warm rain fraction (bottom right plot; Mülmenstädt et al., 2015).

Variable	Stoch	Control	Difference	Relative deviation
$\mathrm{ERFari_{cls}}$ $[\mathrm{W\,m^{-2}}]$	-0.45 ± 0.11	-0.29 ± 0.09	-0.16 ± 0.14	57%
ERFaer $[\mathrm{W\,m^{-2}}]$	-1.52 ± 0.16	-1.45 ± 0.21	-0.07 ± 0.27	5%

	Present-Day		Pre-Industrial	
Variable	Difference	Relative deviation	Difference	Relative deviation
SW_{net} $[\mathrm{W\,m^{-2}}]$	-0.34 ± 0.22	$-0.15\,\%$	-0.47 ± 0.19	$-0.20\,\%$
$SW_{\mathrm{net,cls}}$ $[\mathrm{W\,m^{-2}}]$	-0.22 ± 0.07	$-0.08\,\%$	-0.13 ± 0.06	$-0.05\,\%$
LW_{net} $[\mathrm{W\,m^{-2}}]$	0.06 ± 0.14	$0.03\,\%$	0.26 ± 0.17	$0.10\,\%$
$LW_{\mathrm{net,cls}}$ $[\mathrm{W\,m^{-2}}]$	0.04 ± 0.09	$0.02\,\%$	0.11 ± 0.10	$0.04\,\%$
TCC $[\%]$	-0.08 ± 0.14	$-0.13\,\%$	0.17 ± 0.14	$0.26\,\%$
AOD	0.009 ± 0.002	$7.8\,\%$	0.006 ± 0.002	$6.0\,\%$
ω_{KS}	0.015 ± 0.003	$2.64\,\%$	0.014 ± 0.005	$2.42\,\%$
ω_{AS}	$(1.1 \pm 0.4) \cdot 10^{-3}$	$0.11\,\%$	$(0.9 \pm 0.6) \cdot 10^{-3}$	$0.10\,\%$
ω_{CS}	$(0.03 \pm 0.05) \cdot 10^{-3}$	$0.003\,\%$	$(0.05 \pm 0.15) \cdot 10^{-3}$	$0.005\,\%$
σ_{KS}	$(9.7 \pm 1.0) \cdot 10^{-18}$	$15.1\,\%$	$(8.0 \pm 1.1) \cdot 10^{-18}$	$14.3\,\%$
σ_{AS}	$(20.8 \pm 6.9) \cdot 10^{-15}$	$4.5\,\%$	$(22.7 \pm 7.2) \cdot 10^{-15}$	$4.8\,\%$
σ_{CS}	$(0.69 \pm 0.07 \cdot 10^{-12}$	$3.9\,\%$	$(0.71 \pm 0.07) \cdot 10^{-12}$	$4.0\,\%$
α	$(-0.8 \pm 11.5) \cdot 10^{-3}$	$-0.11\,\%$	$(6.4 \pm 13.8) \cdot 10^{-3}$	$0.94\,\%$

Table 1. Changes of global mean values of optical and radiative variables due to the implementation of subgrid-scale variability of clear-sky relative humidity are listed. Uncertainties of the mean value are calculated for a 95 %-confidence interval on basis of yearly mean values

from the temporal variability. Uncertainties of differences are added in quadrature. ω is the single scattering albedo and σ the effective extinction cross section. The indices KS, AS and CS stand for Aitken, Accumulation and Coarse mode. α is the Ångström exponent, SWnet the net short waveradiation and with index SWnet,cls the net short wave radiation in the clear-sky part. With the same meaning for the indices LW is the longwave radiation. TCC is the total cloud cover. Results are presented for present-day and pre-industrial emissions.